



A Portable Microscale Cell Culture System with Indirect Temperature Control

Citation

Mäki, A. J., Verho, J., Kreutzer, J., Ryyänen, T., Rajan, D., Pekkanen-Mattila, M., ... Kallio, P. (2018). A Portable Microscale Cell Culture System with Indirect Temperature Control. *SLAS Technology*, 23(6), 566-579. <https://doi.org/10.1177/2472630318768710>

Year

2018

Version

Peer reviewed version (post-print)

Link to publication

[TUTCRIS Portal \(http://www.tut.fi/tutcris\)](http://www.tut.fi/tutcris)

Published in

SLAS Technology

DOI

[10.1177/2472630318768710](https://doi.org/10.1177/2472630318768710)

Take down policy

If you believe that this document breaches copyright, please contact cris.tau@tuni.fi, and we will remove access to the work immediately and investigate your claim.

A Portable Microscale Cell Culture System with Indirect Temperature Control

Antti-Juhana Mäki^{†*}, Jarmo Verho[†], Joose Kreutzer[†], Tomi Ryynänen[†], Dhanesh Rajan[†], Mari Pekkanen-Mattila[‡], Antti Ahola[†], Jari Hyttinen[†], Katriina Aalto-Setälä[‡], Jukka Lekkala[†], and Pasi Kallio[†]

[†]BioMediTech Institute and Faculty of Biomedical Sciences and Engineering, Tampere University of Technology, Korkeakoulunkatu 3, 33720 Tampere, Finland

[‡]BioMediTech, Faculty of Medicine and Life Sciences, University of Tampere, Lääkärintie 1, 33014 Tampere, Finland

*Corresponding author, Email: antti-juhana.maki@tut.fi

Keywords

feedback control, microfluidics, modeling, temperature, cell culture

Abstract

A physiologically relevant environment is essential for successful long-term cell culturing *in vitro*. Precise control of temperature, one of the most crucial environmental parameter in the cell cultures, increases the fidelity and repeatability of the experiments. Unfortunately, direct temperature measurement can interfere with the cultures or prevent imaging of the cells. Furthermore, the assessment of dynamic temperature variations in the cell culture area is challenging with the methods traditionally used for measuring temperature in cell culture systems. To overcome these challenges, we integrated a microscale cell culture environment together with a live-cell imaging and a precise local temperature control that is based on an indirect measurement. The control method uses a remote temperature measurement and a mathematical model for estimating temperature at the desired area. The system maintained temperature at $37\text{ }^{\circ}\text{C} \pm 0.3\text{ }^{\circ}\text{C}$ for over four days for over four days. We also showed that the system precisely controls the culture temperature during temperature transients and compensates for the disturbance when changing the cell cultivation medium, and presented the portability of the heating system was presented. Finally, we demonstrated a successful long-term culturing of human induced stem cell-derived beating cardiomyocytes, and analyzed their beating rates in different temperatures.

Introduction

Cell culturing *in vitro* is one of the cornerstones of modern biology. It is known that mammalian cells are very sensitive to the properties of their environment; for example, temperature, oxygen concentration, mechanical stimulation, and pH. Therefore, it is crucial to provide a proper microenvironment for successful long-term cell culturing. Furthermore, a physiologically relevant cell culture environment is key for achieving the reliable data required in, for example, stem cell-based disease modeling studies.^{1–6}

Compared to traditional cell culturing methods using bioreactors, the use of microfabricated microfluidic systems is a fascinating approach due to its better control over the physiological culturing conditions.^{7–9} Other advantages of using these devices are their faster response times, lower fabrication costs and power requirements, and smaller reagent consumptions. Even though several commercial microbioreactors exist, they are typically expensive, do not provide uniform environmental conditions for cells, and have only a limited number of designs available.^{10–12} Therefore, there have been many studies on creating cost-effective microbioreactors for cell cultures *in vitro*. Typically, these devices are fabricated from polydimethylsiloxane (PDMS) using a so-called soft lithography technique, due to this being an easy, fast, and cheap fabrication method. Furthermore, because PDMS is transparent, bio-compatible, and gas permeable, it is well suited for cell culturing systems.^{4,5,13–17}

Proper temperature is one of the most important microenvironmental parameters in cell culturing as the intrinsic properties of fluids and cells are affected by temperature variations. Hence, temperature should be controlled carefully to provide optimal circumstances for cell growth and differentiation.¹⁸ It has also been showed that temperature has a strong effect on the emergent network activity and membrane potential at the cellular level.¹⁹ Precise control of the environmental temperature was required for microrheology measurements; activity of the cells

slowed and they became softer when the temperature was lowered.²⁰ However, several methods and techniques used in cell culturing cause temperature variations in the culture. For example cardiac cell research can include such analysis methods as patch clamp, multielectrode arrays, fluorescent imaging, impedance assays, video microscopy, and live-cell imaging, to name a few.²¹ During the culturing, it is common to move the cultured cells from one measuring instrument to another; for instance, from the incubator to live-cell imaging and analysis. Unfortunately, without a proper portable heating system, these movements of the cell cultures can create significant temperature variations to the cultures, resulting unwanted stimulations to the cells. Therefore, a control system that can minimize temperature variations is very important to successfully culture cells *in vitro*. Another potential source of temperature variations is the change of the cell culture medium which is typically performed every 2-3 days. If the medium is not carefully pre-conditioned, the medium change can cause a temperature stress to the cells.

A typical problem with the accurate temperature control is that it requires a precise temperature measurement from the cell culture. This direct measurement brings some challenges; for example, the sensor can interfere with the cells and prevent microscopic inspection. In many cases, it is significantly more difficult to place sensors in the region of interest than elsewhere; for example, outside the cell culture chamber. Also, if one is placing the temperature sensor inside the chamber, close to the cells, a larger cell culture chamber is often required.^{2,10} Therefore, an indirect temperature measurement is preferable to a direct measurement in the cell area.

Temperature sensors have been placed outside the chamber in many cell culture studies. Solutions include placing sensors together with the heating element,²²⁻²⁴ close to the inlet of the chip or the culture chamber,^{25,26} downstream and upstream from the culture chamber,²⁷ or next to the device.²⁸ However, none of these cases can guarantee the exact temperature of the cell area. Typically reported temperature differences between the measured temperature and the temperature

of the cell area have been up to 2 °C–3 °C.²⁸ This difference is typically too large for cell culture studies.^{19,21,29} For instance, it was shown that temperature variation between 37 °C and 39 °C altered cardiomyocyte beating characteristics.²¹ Also, the firing rate during up states in the cortical network was modulated when temperatures varied between 36 °C and 38 °C.¹⁹ To minimize temperature variations, a sensor has been placed in a separate reference chamber;^{30–32} however, this method requires more space as one chamber is used only for temperature logging. An extremely good insulating system is required for precise temperature control using only a sensor placed outside. One demonstrated solution to provide a uniform temperature profile has been to build a complex, large insulated device in which a water bath surrounds the chamber.^{19,32,33} Unfortunately, this typically leads to a longer temperature settling time during the heating phase, such as approximately 60 min,³² or a minimum time of 5 min to change temperature by 1 °C.¹⁹ Moreover, with this technique it can still be difficult to avoid excessively large temperature differences between the central part of the chamber and the surrounding parts.¹⁰

Optical methods have also been proposed for measuring temperature locally. Measurement from the cell culture area using infrared cameras is challenging because the PDMS material shields these signals.³⁴ Fluorescent labels have been used for direct temperature measurement in microfluidic devices.^{35–37} With this method, fluorescent dyes are mixed into the working fluid. Although the method can be used with glass-based materials, it presents significant problems with porous materials, such as PDMS, because accurate temperature measurements are prevented by the adsorption of dye particles into the material. Some solutions have been demonstrated to overcome this adsorption problem.³⁵ however, measurement performance is still reduced. Furthermore, typical temperature measurement precision (approximately 2.5 °C at 37 °C³⁶) is not sufficient for cell culture studies.

To solve the aforementioned problems, we previously developed an indirect temperature measurement method to monitor temperature in the cell culture area using a system identification approach.³⁸ We used a commercial heater and a cell culture device made in-house, and showed that our method precisely estimated the cell culture temperature. We also presented a simulation study to demonstrate how the method could be used for temperature control purposes. In this study, we extend this approach by integrating an indirect temperature control into a developed cell culture system. The control method combines an external temperature measurement and a numerical model to calculate an approximation of the temperature at the desired location. This estimate is then compared to the desired temperature set-point, thereby providing an indirect measurement and control method for the cell culture temperature. Furthermore, the developed heating system is portable; it has a power source to maintain the desired temperature for over one hour for applications where transportation of the system is needed. The system is also suitable for a long-term microscopy and cell imaging, as it includes a gas supply for the maintenance of the proper carbon dioxide (CO₂) and oxygen (O₂) concentrations in the cell culture media.

In this study, we show how accurate temperature in the cell culture area can be performed without disturbing the cells or preventing imaging. First, we demonstrate how the heating system compensates disturbances arising from the ambient room temperature variations. We also illustrate how the cell culture temperature is restored to the desired level after opening of the device or liquid change. Finally, using beating cardiomyocytes, we demonstrate a successful long-term cell culturing and a temperature stress-study.

The rest of the paper is organized as follows. First, it explains the working principle of the system, describes details on the experimental setups used, and presents developed models. Experimental data and control results are given next; the models are developed, their performances are compared to the measured data, and finally experiments with the developed closed-loop control

system are presented. Then, the results from this paper are discussed, before providing conclusions and possible future work.

Materials and Methods

The main components of the cell culture system are an indium tin oxide plate (ITO) as a heating element ($70 \text{ mm} \times 70 \text{ mm} \times 0.7 \text{ mm}$ boro-aluminosilicate glass plate from UniversityWafer, Inc., Boston, MA, USA, with a resistivity of $8\text{-}10 \text{ } \Omega/\text{sq}$), a temperature sensor plate (TSP) made in-house on a glass substrate ($49 \text{ mm} \times 49 \text{ mm} \times 1 \text{ mm}$ from Gerhard Menzel GmbH, Braunschweig, Germany), and a cell culture device made in-house. A Pt100 sensor attached on the ITO plate was used to measure the heater temperature (T_{ITO}), and spring contacts were used to connect the TSP pads as shown in Fig. 1.

Working Principle of Indirect Temperature Control

The temperature estimate is made using a mathematical model and a temperature measurement; the measured temperature outside the desired location ($T_{outside}$) is supplied as an input to the mathematical model. The model calculates an estimate of the cell culture temperature, $T_{cell-est}$, which is compared to the set-point temperature, T_{set} , to complete the closed-loop feedback system, as shown in Fig. 2. In the control system, we implemented a proportional-integral-derivative (PID) controller. In this study, however, we used only a proportional-integral (PI) controller with such parameters ($P = 1.7$, $I = 0.03$) that the control system had a close-to-critically damped response with only a minor overshoot. Output power of the controller was limited to values between 0 and 2 W. As there was no active cooling included, the temperature decrease was entirely based on heat dissipation. For the model development and analysis, we also monitored the ambient room temperature T_{room} , and the real cell culture temperature, T_{cell} , and compared the estimated and

measured cell culture temperatures. It should be emphasized that T_{cell} was only used to verify the temperature estimate results, and was never used for temperature control purposes.

We developed two temperature estimation models for different purposes. The difference between the models was that different measurements were used as $T_{outside}$. Model 1 was based on measured ITO heater temperature using a Pt100 sensor glued onto the ITO plate (see Fig. 1). For this reason, $T_{outside}$ is marked as T_{ITO} in Model 1. In Model 2, we measured the temperature using the TSP with a sensor located close to the cell culture area; therefore, $T_{outside}$ is marked as T_{TSP} in Model 2. The TSP will be presented in more detail in Fig. 3.

The sensor required in Model 1 is easy to place, and the location of the sensor can be chosen rather freely. Also, there is no need to use the sensor plate for temperature control. However, as this method does not measure temperature inside the cell culture chamber, the estimated temperature is less accurate. Therefore, Model 1 is not capable of fully compensating for temperature changes inside the chamber caused by, for instance, variations in the ambient room temperature. Furthermore, this approach does not work properly in cases when the temperature inside the culture chamber changes without changes in T_{ITO} . The example of opening the device and changing the liquid inside the chamber is presented in Results section and in Fig. S6.

For the aforementioned reasons, we also developed Model 2, which measures the temperature inside the chamber close to the cell culture area and therefore can better predict temperature changes in the cell area. Model 2 can compensate for the residual thermal disruptions caused by microscopy imaging and changes in the ambient temperature, both of which the cell culture temperature. The drawbacks of this approach are that the sensor is typically more fragile, the sensor is more difficult to position as it needs to be in a certain location, and the sensor plate is required. To summarize, the two models have their preferred applications depending on the requirements.

Experimental Setups

Overall Device Description

The measurement system included the ITO heater, TSP, PDMS-based cell culture device, gas supply, illumination and optics, frames and stages, and electronics required for temperature measurement and control. We designed all the custom-made mechanical parts in the setup using SolidWorks (SolidWorks, Cambridge, UK). The setup is shown in Fig. 1, which also includes the cell imaging arrangement. The cell imaging was carried out using an invert-upright convertible compact microscopy system as previously described.³⁹ In our case, prior to time-lapse video microscopy (20X, 1.3 MP camera -BFLY-U3-13S2M-CS, Point Grey Research, Inc., Richmond, BC, Canada), initial sample positioning and coarse focusing were performed using system's manual xyz-stage. Precise focusing and timely focus corrections in long-term microscopy were carried out with the motorized focusing stage. A custom written MATLAB (MathWorks, Inc., Natick, MA, USA) user interface software was implemented for controlling the illumination, stage heater and time-lapse data logging (uncompressed .avi videos with frame-rate of 50 frames per second and temperature sensors).³⁹

Electronic circuits made in-house (Fig. S1), were designed to connect the TSP and the heater to the computer and to the external power source, unless a battery mode was used. The main design criteria for the heating controller electronics were low cost, relatively small size, capability of running the model-based temperature control algorithms and the aforementioned option for short-term (but over an hour) battery operation. The basic measurement principle is shown in Fig. S1. Due to the low and relatively constant wiring resistances, a simple two-wire ratiometric measurement method was chosen. The rather low reference voltage (200 mV) was a compromise between sensor self-heating, resolution, noise, and the sensitivity to thermoelectric offset voltages. A 16 bit resolution of the chosen analog-to-digital converter (ADC; LTC2486 from Analog

Devices, Inc., Norwood, MA, USA) results in approximately 12 mK temperature measurement resolution, which is more than sufficient and below the noise floor. Two identical 100 Ω reference resistors were used to cancel the effects of the input current of the ADC.

While the diagram shows only one channel, the device has two channels, allowing the user to easily switch between two different temperature feedback locations. This simple arrangement designed for the Pt100 sensor was not sufficient for the TSP sensors, as they can have significant and varying wiring and contact resistances. To support the use of the TSP sensors, the circuit was modified to a four-wire measurement compensating for the wiring resistance, as shown in Fig. S1. This arrangement requires the use of both ADC channels, allowing only one four-wire measurement instead of two two-wire measurements.

In order to minimize the interference caused by the heating element current, a constant current drive scheme was adopted (Fig. S1). While a fully linear driver would have been preferable from the interference point of view, the excessive power dissipation of such a driver made it impractical. Thus, a switching voltage-controlled current source (LT3477, Analog Devices, Inc.) was chosen. The control input comes in the form of a pulse-width modulated signal, which is filtered to produce a direct current (DC) control signal for the current source. While it can be assumed that some of the switching noise of the current source reaches the ITO plate, at least the amplitude is low and the frequency is well above typical biosignal frequencies.

The actual controller was built around an 8 bit microcontroller (ATMega328, Microchip Technology, Inc., Chandler, AZ, USA), which measures the sensor resistances, performs simple gain and offset compensations, and converts the results to temperatures either by using a standard (second-order) Pt100 equation or by using a user-entered, first-degree polynomial fit. This temperature reading is supplied either directly or through the identified model to the PID controller. The temperature measurement, identification and PID controller run at a 5 Hz frequency. The

device has a USB port for configuring the device and for logging temperature data. It also contains a 3.1 Ah, 18650-size lithium ion battery and an associated USB charger (LTC4098, Analog Devices, Inc.).

Heating System

A heating system that provides a uniform temperature profile is very important for successful indirect temperature control and long-term cell culture studies. Also, optical microscopy is typically required in these studies. Therefore, an ITO plate was chosen as a heating element, as it is not only electrically conductive but also optically transparent; Joule heating can be generated when electrical power is applied, and at the same time, ITO does not obscure illumination. To supply the heating current uniformly over the ITO plate, and thus to equalize temperature on top of the plate, we e-beam evaporated copper pads 900 nm thick ($3.5\text{ mm} \times 70\text{ mm}$) onto the ends of the ITO plate. These copper lines are shown in Fig. 1(a). Furthermore, a 300 nm silicon nitride (Si_3N_4) insulator layer was deposited over the ITO using a plasma-enhanced chemical vapor deposition (PECVD) process.

Frame Design

A proper design of the frame (see Fig. 1, item 5) for the ITO plate is important for achieving a uniform temperature profile. We tested three different frame structures. Frame 1, manufactured by Saloteam Oy (Salo, Finland), was made of aluminum and mounted to an xyz-stage (see Fig. 1, item 7a). However, non-uniform heating with large temperature gradients on the plate was observed with this frame. Therefore, we designed and 3D-printed a frame with the same dimensions but made from polylactic acid (PLA); this was Frame 2. We observed remarkably reduced temperature gradients with Frame 2. To further improve the uniformity of the temperature, a 3-mm-thick plate of thermally insulated material (Finnfoam plate from Finnfoam Oy, Salo, Finland) was added between the ITO glass and Frame 2. The outer dimensions of the insulation

plate were 70 mm × 70 mm with a hole of approximately 62 mm × 62 mm in the middle. The combination of Frame 2 and the thermal insulator layer was Frame 3.

To compare the temperature distribution in the different frames, we used thermal imaging. As direct thermal imaging of the ITO glass was not possible due to reflection issues, we placed a glass plate (50 mm × 50 mm × 0.5 mm) on top of the ITO plate and only considered temperature measurement on this area of the plate (marked with dashed rectangles in Fig. S2). We first heated the ITO plate such that T_{ITO} (based on the sensor reading as presented in Fig. 1(a)) was stabilized to 34 °C. Then, thermal images were taken from the three frames using a Flir One thermal camera (FLIR Systems, Inc., Seattle, WA, USA). Temperature profiles in this region were further analyzed, and the results are summarized in Table S1.

It is clear from Table S1 that temperature gradients were significantly reduced with Frame 3 when compared to Frame 1. This is an important result, as temperature differences inside the cell culture chamber should be minimized to provide as equal temperature as possible for every cell in the culture. In the table, T_{min} , T_{max} , T_{avg} , $T_{max} - T_{min}$, and $T_{max} - T_{avg}$ are minimum, maximum, and average measured temperatures, difference between the maximum and minimum temperatures, and difference between the maximum and average temperatures, respectively.

Temperature Sensor Plate

We designed the TSP for logging the temperature inside the cell culture chamber. The TSP was built on a glass plate and included 14 identical temperature sensors as shown in Fig. 3. The TSP consisted of resistors, tracks, and contact pads patterned using photolithography on an e-beam evaporated copper layer that was 275 nm thick. The resistor and the track area were electrically insulated using 100 nm silicon dioxide (SiO₂) and 500 nm Si₃N₄ layers with PECVD. The width of the resistor line in the design was 20 μm.

Temperature sensors were calibrated in a temperature-controlled oven by measuring their electrical resistances using a four-wire method at several different temperatures from 24 °C to 38 °C after the plate was thermally stabilized. A typical room-temperature resistance was approximately 105 Ω . As a good linear relationship between electrical resistance and temperature was obtained, a linear interpolation was used to estimate temperature from the measured resistance.

Cell Culture

The cell culture device, its fabrication procedure, and the main working principle has been described previously.³⁹⁻⁴¹ Therefore, we present here only the main steps and details of study-specific differences. The design goals were to enable on-line microscopy (therefore, transparent materials were chosen) and to keep the cell culture alive for several days in the cell culture device.

The structure of the cell culture device is shown in Fig. 1(c) with three main parts: a cell culture chamber, a lid, and a cover. The lid was machined from polycarbonate (PC; Saloteam Oy), and the cover was 3D printed (from Shapeways, Eindhoven, the Netherlands). The lid made a watertight seal on the culture chamber and prevented contamination from entering the chamber. This setup also enabled the use of a dry gas supply without significant evaporation of the culture medium. The same technology has been shown to keep the cell culture alive and vivid outside an incubator over three days.⁴¹

The cell culture chamber was cast in-house from PDMS (Sylgard 184 from Dow Corning, Auburn, MI, USA) using standard soft-lithography techniques. Cells were plated on a round opening area (diameter of 10 mm) that was punched in the bottom of the chamber. During experiments, the cell culture chamber was reversibly bonded on the TSP and filled with 1 mL deionized water or cell culture medium before the chamber lid was closed. The desired gas environment is provided to the cell area by covering the cell culture chamber by the cover. With the cover placed atop the lid and the chamber, the gas supply pipe was connected to provide the

desired gas environment (CO₂ and O₂ concentrations) inside the chamber. In cell culture studies, we used a motorized inverted microscopy system, made in-house,³⁹ for cell imaging as described previously.

Cardiomyocytes (CMs) derived from the human induced pluripotent stem (iPS) cell line UTA.04602WT, as described previously,⁴² were cultured in the developed system. Differentiated beating iPS-CMs were used in the present study. The iPS-cells, derived from a healthy person, have been differentiated into cardiomyocytes with the standard method used in our laboratory. The differentiated iPS-CMs have been characterized with multiple molecular biology and functional methods and the characterization data have been published in our earlier studies.⁴³⁻⁴⁵ For sterilization, TSPs were immersed in 70% ethanol and dried under sterilized conditions. The PDMS culture chamber was mounted directly on the sterilized TSP. The beating iPS-CM aggregates were plated at the bottom of the cell chamber, which was first hydrophilized with fetal bovine serum (FBS) and then coated with 0.1% gelatin type A (Sigma-Aldrich, St Louis, MO, USA). The iPS-CMs were cultured in KO-DMEM-media (Lonza, Basel, Switzerland) with 20% FBS (Lonza), 1% non-essential amino acids (Cambrex, East Rutherford, NJ, USA), 2 mM Glutamax (Invitrogen, Carlsbad, CA, USA), and 50 U/mL penicillin/streptomycin (Lonza). For each cell chamber, three to four iPS-CM aggregates were plated. After plating, the iPS-CM aggregates were cultured for 24 h in an incubator (37 °C, 5% CO₂, 19% O₂, 76% N₂) for initial stabilization. After that, the device was removed from the incubator, closed with the lid and the cover, and placed on the preheated (37 °C) ITO heater. The gas environment around the cell culture area was created by flushing with a gas mixture (5% CO₂, 19% O₂, 76% N₂) at a constant flow rate of 5 mL/min.

Temperature Estimation Models

In the study, we used a so-called black-box technique to develop models using only input and output data, regardless of the physical system.⁴⁶ We used a prediction error⁴⁷ that made a prediction that is as close as possible to the true system if it was known, to develop our models. We compared models using a fit number, which is based on a normalized root-mean-square error criterion. It can be calculated (as a percentage) using the following equation:⁴⁸

$$fit = 100 \left(1 - \frac{\|y - \hat{y}\|}{\|y - \bar{y}\|} \right) \quad (1)$$

where y and \hat{y} are the measured and the estimated output, respectively, and \bar{y} is the mean of y . We used input and output data, presented in Fig. 4, to develop the models. We used MATLAB R2016a together with System Identification Toolbox (the MathWorks, Inc.) to derive discrete-time, state-space models. The models include a state variable vector $x(k)$, an input variable vector $u(k)$, and an output variable vector $y(k)$, and have the following structure:⁴⁸

$$\begin{aligned} x(k+1) &= Ax(k) + Bu(k) \\ y(k) &= Cx(k) + Du(k) \end{aligned} \quad (2)$$

where matrices A , B , C , and D represent a state matrix, an input-to-state matrix, a state-to-output matrix, and a feed-through matrix, respectively. These matrices are defined using measurements, presented in Fig. 4, for both models that are developed in this study.

Results

Model Development

To develop the temperature estimation models, temperature was controlled using $T_{outside}$. In the experiments, the set-point temperature was randomly changed, and both $T_{outside}$ and T_{cell} were recorded. Fig. 4(a) presents measurements for T_{ITO} (Model 1) and Fig. 4(b) for T_{TSP} (Model 2). Initially, we tested second-order state-space models, but the accuracies of the temperature

estimates were not acceptable, especially for Model 1; therefore, we used third-order models, with the following structure:

$$A = \begin{bmatrix} a_{11} & a_{12} & 0 \\ 1 & 0 & 0 \\ 0 & 1 & 0 \end{bmatrix}, B = \begin{bmatrix} 1 \\ 0 \\ 0 \end{bmatrix}, C^T = \begin{bmatrix} c_1 \\ c_2 \\ c_3 \end{bmatrix}, D = 0 \quad (2)$$

As the coefficient of the matrix D was zero, no direct or linear relation between the input and the output was detected. We determined constants a_{11} , a_{12} , c_1 , c_2 , and c_3 using $T_{outside}$ and T_{cell} as input and output signals, respectively, in the system identification process. We obtained the following parameter values for the models:

- Model 1: $a_{11} = 1.99$, $a_{12} = -0.99$, $c_1 = 0.33$, $c_2 = -0.66$, and $c_3 = 0.33$
- Model 2: $a_{11} = 1.19$, $a_{12} = -0.20$, $c_1 = 0.52$, $c_2 = 0.58$, and $c_3 = 0.06$

The measured temperatures and the temperatures simulated using the models with the aforementioned parameter values are compared in Fig. 4(c) and 4(d). The calculated model fit numbers were 94.2% and 94.8% for Model 1 and Model 2, respectively, indicating that the models are suitable for estimating the cell culture temperature. In the following sections, we use the outputs of these models – the estimated temperatures ($T_{cell-est}$) – for controlling the cell culture temperature. In the next section, we will illustrate the usefulness of the indirect control system.

Comparison of Different Control Strategies to Maintain Constant Temperature

In this section, we compare different controller strategies to illustrate the benefits of the developed indirect control system. As mentioned, to obtain optimal cell growth and differentiation, precisely controlled temperature is required. Therefore, the purpose of this experiment is to show, how variations in the ambient room (marked as T_{room}), if improper control system is used, will

produce undesired changes in the cell culture temperature (T_{cell} , see Fig. 5). We implemented one open-loop and three closed-loop control systems to compare different controller strategies.

In the open-loop system, a constant heating power was used; no measurement was used to control the heating power. Three closed-loop systems used the same PI controller ($P = 1.7$, $I = 0.03$), but the control was based on different signals in the feedback loop (see Fig. 2). In the first closed-loop system, temperature was regulated based on the measured temperature of the ITO heater T_{ITO} (from the glued Pt100 sensor, marked with a red rectangle in Fig. 1(a)), whereas the control of the second closed-loop system was based on T_{TSP} . This sensor is located on the TSP, and is marked with a green circle in Fig. 3. The last control system used the combination of T_{TSP} and Model 2; the control was based on the estimated $T_{cell-est}$ as explained previously.

In the begin of each experiment, we added 1 mL deionized water to the cell culture chamber and pre-heated the system so that T_{cell} was close to 37 °C before we started to record T_{room} and T_{cell} for 15 hours. Results using different controller strategies are shown in Fig. 5. Implemented controller strategies provided significantly different results during the 15-hour long experiments as shown in Fig. 5. Maximum variations in the measured T_{cell} during the experiment were 1.5 °C (open-loop), 1.0 °C (closed-loop using T_{ITO}), and 0.2 °C for the closed-loop systems using T_{TSP} or $T_{cell-est}$. Clearly, use of the open-loop system or the first closed-loop control system based on T_{ITO} are not recommended for the temperature control as changes in the ambient air had high impact on T_{cell} . Remarkable better control results were achieved by using T_{TSP} or the developed model-based temperature estimation as a feedback signal.

Precise Long-Term Temperature Control

Indirect control system provided very good results as presented in the previous section. Therefore, a long-term temperature control test was performed. The purpose is to support long-

term cell growth by precisely regulating the cell culture temperature was to 37 °C. We again added 1 mL deionized water to the cell culture chamber and calculated $T_{cell-est}$ using Model 2 and the measured T_{TSP} . We also monitored the real temperature, T_{cell} , and compared the estimated and measured cell culture temperatures. During the experiment, the measured ambient room temperature, T_{room} , varied between 22.6 °C and 25.9 °C. The results in Fig. 6 show that the cell culture temperature was maintained at $37\text{ °C} \pm 0.3\text{ °C}$ for more than four days. It should be noted that a sensor connection problem at approximately 10 h created artificial noise in the measured signal shown in Fig. 6. The system capability of compensating the environmental variations is demonstrated in Fig. S3. It presents how T_{room} and the controller output power are changed during the experiment. As mentioned, there are some variations in T_{cell} ($37\text{ °C} \pm 0.3\text{ °C}$); however, these are more related to model inaccuracies and simplifications than environmental variations, which are compensated by the controller. This is presented in Fig. S3; when the measured temperature indicates a temperature change in the ambient air (T_{room}), the controller modifies the heating power to compensate this change. It should be emphasized that T_{room} was only used for the monitoring purposes, not directly in the control loop.

Controlled Temperature Steps

A precisely controllable cell culture temperature provides several opportunities for temperature-dependent cell behavior studies. For example, it enables one to characterize transient behaviors of the cell cultures during the heating and cooling phases around the physiological temperature,² or to determine a temperature threshold for the activation of ion channels.⁴⁹ Our system can precisely monitor and control cell culture temperature, T_{cell} , during temperature transients, as shown here. The results using Model 1 are shown in Fig. 7(a). The average temperature estimation error was 0.40 °C (see Fig. S4). Figure 7(b) demonstrates temperature control in temperature transients using

Model 2. As this model uses T_{TSP} for $T_{cell-est}$, a temperature measured at a location that is much closer to the desired area than the location used in Model 1, the results are significantly better; the average temperature estimation error dropped to 0.21 °C (see Fig. S5). As these estimation errors are acceptable in cell culture studies, these results demonstrate that the proposed system can be used in temperature-dependent cell tests, such as cell stress tests.

Disturbance Compensation During Liquid Changes

The performance of the temperature control system during a liquid change, mimicking the change of a cell culture medium, is demonstrated using Model 2. Here, we changed liquid that was heated to 37 °C with liquid stabilized to the ambient air temperature (approximately 24 °C). This is an extreme case; in a typical application, the fresh cell cultivation liquid would be close to 37 °C. Therefore, this demonstration overemphasizes the effect of a typical temperature drop, thus imposing a higher requirement on the heating system. As Model 1 uses the temperature measured from the ITO heater, the result with Model 1 would not have been satisfactory, because the temperature mainly changes inside the cell culture chamber.

The results (Fig. S6) show how the system compensates for the temperature drop caused by changes in the liquid temperature. Figure S6(b) shows a time period just before and after the second liquid change; the cell culture chamber was opened at approximately 53 min. Because of this, the temperature in the cell culture area started to drop, as measured by the sensor (T_{TSP}), and the controller started to compensate for this drop by increasing the heating power as shown in the inset in Fig. S6(b). At 54.5 min, the system restored T_{cell} to 37 °C, before the liquid was changed at 55 min. This demonstrates that the system can maintain the temperature regardless of the typical temperature variations that occur during cell culturing.

Portable Heating System

In the case of the portable heating system, which would be beneficial while moving the device, the temperature control was directly based on T_{ITO} . Using a battery-operated system, we maintained and precisely controlled the temperature of the ITO heater over an hour at 37 °C (Fig. S7). Therefore, for example live-cell imaging can be performed in a constant temperature, without providing undesired temperature stimulation to the cell culture.

Cell Experiments

To demonstrate the capability of the system for long-term cell culturing *in vitro*, the iPS-CM aggregates were cultured in the system, and the beating behavior of the iPS-CMs was assessed for over 100 h. We used Model 1 for temperature control and the imaging system presented in Fig. 1. We recorded 60 s videos with a frame-rate of 50 frames per second, once a day starting 24 h after the cells were initially plated to the device. The iPS-CMs remained functional when cultured in the system; analyzed beating rates on the first day of culturing and 110 h later were 44 and 36 beats per minute (BPM), respectively, using a video image-based method. This non-invasive method, presented by Ahola *et al.*⁴⁴ has been proved to be a reliable and fast approach to monitor the mechanical beating behavior of cardiomyocytes.²¹ Snapshot images of the initial and final videos are presented in Fig. S8 (see supplementary material for more information and the recorded videos). These results demonstrate the suitability of the device for a long-term cell culturing of iPS-CMs.

Another set of the iPS-CM aggregates were exposed to different temperatures. We varied temperature between 37 °C and 25 °C in several steps. We waited 25 minutes before a video recording to stabilize the cell culture temperature. After experiment, using the same video image-based analysis,⁴⁴ we calculated the beating rates in different temperatures. The results are shown

in Fig. 8. As can be seen in Fig. 8(a), we were able not only to change the beating rate of the cardiomyocytes, but also to recover the beating rate when the temperature was returned to 37 °C. The calculated average beating rate at 37 °C was $54.8 \text{ BPM} \pm 3.2 \text{ BPM}$ based on 11 measurements points presented in Fig. 8(b). Furthermore, average beating rates at 35 °C and 34 °C were 44.5 BPM and 36.0 BPM, respectively; however, it should be highlight here, that these latter results are only from four measurement points, and more comprehensive studies are required.

Using the recorded videos, we further parameterized the contractile motion of the iPS-CM aggregates using previously presented method with Fridericia QT correction.^{50,51} In brief, the motion is characterized by three parameters related to the widths of the contraction transient peaks at different heights, as presented in Fig. 8(c). The widths are defined at the heights of 10%, 50% and 90% from the transient maximum. The results shown in Fig. 8(d) demonstrate the temperature dependence of the contractile motion. The results also show that cells return to their normal beating mechanics after the stress induced by the temperature change. Finally, these results highlight the importance of maintaining a stable temperature during cell experiments, as temperature fluctuations influence the contraction durations.

Discussion

We demonstrated a microscale cell culture device together with a unique indirect temperature control method. To our best knowledge, this is the first time that the cell culture temperature has been precisely maintained and regulated without measuring the temperature directly from the cell culture area. Especially, our system can precisely control the cell culture during temperature transients without placing a sensor inside the cell culture area; this has typically not been possible in the systems used in previous studies. As a summary, we have demonstrated that the developed system can precisely control the cell culture temperature when *i*) ambient room temperature is changing, *ii*) the system is moved, *iii*) the cell culture device is opened, and *iv*) liquid is changed,

all without direct measurement. Furthermore, the system is suitable for temperature-dependent cell behavior studies; this was demonstrated by studying the beating iPS-CM aggregates.

Our system maintained the temperature at 37 °C for over four days. The measured temperature variation, ± 0.3 °C, was similar to that in other studies; for instance, variations of ± 0.2 °C,^{27,31,32,52,53} ± 0.25 °C,¹⁸ ± 0.26 °C,¹⁰ ± 0.3 °C,⁵⁴ ± 0.4 °C,⁵⁵ ± 0.5 °C,^{56,57} and ± 0.8 °C⁵⁸ have been reported. As the intrinsic properties of fluids and cells are temperature-dependent, it is highly beneficial to prevent large temperature variations in the cell studies. For this reason, it is crucial that the heating system can compensate typical temperature disturbances related to the cell cultures; for example, the variations in the ambient room temperature or the opening of the device and the change of medium. Unfortunately, this is typically not possible with the previously presented devices without direct measurement from the cell culture area, whereas we demonstrated that these disturbances can be indirectly monitored and compensated for using the developed heating system. This allows us to minimize the undesired stimulations of cells origin from the temperature variations. In addition, we presented the portability of the system. With the battery operated heating, a constant cell culture temperature can be maintained for about an hour for instance while moving the device or during live-cell imaging.

With the slight temperature variation of our heating system, a successful cell culture could be carried out. We demonstrated this by culturing the beating iPS-CM aggregates for over four days and using the video image-based beating rate analysis. We also combined this analysis and controlled temperature variations to demonstrate how the beating rate varied in different temperatures. We achieved two main results from this experiment; firstly, we were able to return the beating rate when temperature was set back to 37 °C as is shown in Fig. 8(a). Secondly, even though more tests are needed, the initial results in Fig. 8 clearly show the importance of the precise temperature control. For example, if we consider the closed-loop heating system based on the direct

control of T_{lro} presented in Fig. 5(b), approximately 1 °C temperature differences in the cell area were obtained only because of the variations in the ambient air temperature. This can create unwanted artificial stimulation to the cells; based on the cell experiments, the beating rate of the iPS-CM aggregates was significantly dropped when temperature was decreased from 37 °C to 34 °C. From the average beating rates (54.8 BPM, 44.5 BPM, and 36.0 BPM at 37 °C, 35 °C, and 34 °C, respectively), we can estimate that the beating rate dropped roughly 10% in every °C when temperature was decreased from 37 °C to 34 °C. Even though similar results have been reported,^{59,60} more studies in different temperatures are required to verify our results. Also, for instance the measurement of electrophysiology of the cells in different temperatures using a patch clamp method could be included.

Conclusion

We developed a portable microscale cell culture system device including a precise heating system based on an indirect control method. The method combines a numerical model and a temperature measurement to maintain and control the temperature in the desired area, without the need of placing a sensor in that area. Using the method, we precisely maintained a constant temperature over 100 hours. We also presented accurate temperature control during temperature changes. The model-based control system was also able to compensate for temperature disturbances caused by variations in the ambient temperature, for instance, during liquid changes. Furthermore, we cultured the beating iPS-CM aggregates in the developed system for more than four days. The system was capable of providing a stable and cell-friendly environment for the cell cultures. In addition, a temperature-dependent beating rate was demonstrated with the iPS-CM aggregates.

One future step is to implement oxygen sensing in the system, similar to that presented previously.⁶¹ Integration of a zigzag-shaped heater and a sensor on a single ITO plate could be

possible through conventional photolithography methods.^{55,62} Cell cultures *in vitro* in this study were on a plane. Unfortunately, two-dimensional culture models poorly mimic tissues *in vivo*.⁶³ In the future, designing a three-dimensional cell culture environment would offer a biologically more relevant *in vitro* model and would better reproduce *in vivo* culturing conditions and cell-cell interactions.

Acknowledgment and Funding

This work was supported by Tekes, the Finnish Funding Agency for Technology and Innovation (Decision no. 40346/11), Finnish Culture Foundation, and was carried out within the Human Spare Parts 2 project.

References

1. Chen, H.; Nordon, R. E. Application of Microfluidics to Study Stem Cell Dynamics. In *Emerging Trends in Cell and Gene Therapy*; Danquah, M.; Mahato, R., Eds.; Humana Press: Totowa, NJ, 2013; pp 435–470.
2. Picard, C.; Hearnden, V.; Massignani, M.; et al. A Micro-Incubator for Cell and Tissue Imaging. *Biotechniques* **2010**, *48*, 135–138.
3. Portillo-Lara, R.; Annabi, N. Microengineered Cancer-on-a-Chip Platforms to Study the Metastatic Microenvironment. *Lab Chip* **2016**, *16*, 4063–4081.
4. Velve-Casquillas, G.; Le Berre, M.; Piel, M.; et al. Microfluidic Tools for Cell Biological Research. *Nano Today* **2010**, *5*, 28–47.
5. Kreutzer, J.; Ikonen, L.; Hirvonen, J.; et al. Pneumatic Cell Stretching System for Cardiac Differentiation and Culture. *Med. Eng. Phys.* **2014**, *36*, 496–501.
6. Li, Z.; Fan, Z.; Xu, Y.; et al. Thermosensitive and Highly Flexible Hydrogels Capable of Stimulating Cardiac Differentiation of Cardiosphere-Derived Cells under Static and Dynamic Mechanical Training Conditions. *ACS Appl. Mater. Interfaces* **2016**, *8*, 15948–15957.
7. Whitesides, G. M. The Origins and the Future of Microfluidics. *Nature* **2006**, *442*, 368–373.
8. Macown, R. J.; Veraitch, F. S.; Szita, N. Robust, Microfabricated Culture Devices with Improved Control over the Soluble Microenvironment for the Culture of Embryonic Stem Cells. *Biotechnol. J.* **2014**, *9*, 805–813.
9. Velve-Casquillas, G.; Fu, C.; Le Berre, M.; et al. Fast Microfluidic Temperature Control for High Resolution Live Cell Imaging. *Lab Chip* **2011**, *11*, 484–489.
10. Petronis, S.; Stangegaard, M.; Christensen, C. B. V.; et al. Transparent Polymeric Cell Culture Chip with Integrated Temperature Control and Uniform Media Perfusion. *Biotechniques* **2006**, *40*, 368–376.
11. Chen, C. S.; Jiang, X.; Whitesides, G. M. Microengineering the Environment of Mammalian Cells in Culture. *MRS Bull.* **2005**, *30*, 194–201.
12. Heidemann, S. R.; Lamoureux, P.; Ngo, K.; et al. Open-Dish Incubator for Live Cell Imaging with an Inverted Microscope. *Biotechniques* **2003**, *35*, 708–716.
13. Duffy, D. C.; McDonald, J. C.; Schueller, O. J.; et al. Rapid Prototyping of Microfluidic Systems in Poly(dimethylsiloxane). *Anal. Chem.* **1998**, *70*, 4974–4984.
14. Merkel, T. C.; Bondar, V. I.; Nagai, K.; et al. Gas Sorption, Diffusion, and Permeation in Poly (Dimethylsiloxane). *J. Polym. Sci. Part B Polym. Phys.* **2000**, *38*, 415–434.
15. Ngo, I. L.; Jeon, S.; Byon, C. Thermal Conductivity of Transparent and Flexible Polymers Containing Fillers: A Literature Review. *Int. J. Heat Mass Transf.* **2016**, *98*, 219–226.
16. Young, E. W. K.; Beebe, D. J. D. Fundamentals of Microfluidic Cell Culture in Controlled Microenvironments. *Chem. Soc. Rev.* **2010**, *39*, 1036–1048.
17. Yi, C.; Li, C. W.; Ji, S.; et al. Microfluidics Technology for Manipulation and Analysis of Biological Cells. *Anal. Chim. Acta* **2006**, *560*, 1–23.
18. Fang, C.; Ji, F.; Shu, Z.; et al. Determination of the Temperature-Dependent Cell Membrane Permeabilities Using Microfluidics with Integrated Flow and Temperature Control. *Lab Chip* **2017**, *17*, 951–960.
19. Reig, R.; Mattia, M.; Compte, A.; et al. Temperature Modulation of Slow and Fast Cortical Rhythms. *J. Neurophysiol.* **2010**, *103*, 1253–1261.
20. Picard, C.; Donald, A. The Impact of Environmental Changes upon the Microrheological Response of Adherent Cells. *Eur. Phys. J. E* **2009**, *30*, 127.

21. Laurila, E.; Ahola, A.; Hyttinen, J.; et al. Methods for in Vitro Functional Analysis of iPSC Derived Cardiomyocytes - Special Focus on Analyzing the Mechanical Beating Behavior. *Biochim. Biophys. Acta* **2016**, *1863*, 1864–1872.
22. Saalfrank, D.; Konduri, A. K.; Latifi, S.; et al. Incubator-Independent Cell-Culture Perfusion Platform for Continuous Long-Term Microelectrode Array Electrophysiology and Time-Lapse Imaging. *R. Soc. Open Sci.* **2015**, *2*, 150031.
23. Habibey, R.; Golabchi, A.; Latifi, S.; et al. A Microchannel Device Tailored to Laser Axotomy and Long-Term Microelectrode Array Electrophysiology of Functional Regeneration. *Lab Chip* **2015**, *15*, 4578–4590.
24. Jang, J. M.; Lee, J.; Kim, H.; et al. One-Photon and Two-Photon Stimulation of Neurons in a Microfluidic Culture System. *Lab Chip* **2016**, *16*, 1684–1690.
25. Wang, K. I.-K.; Salcic, Z.; Yeh, J.; et al. Toward Embedded Laboratory Automation for Smart Lab-on-a-Chip Embryo Arrays. *Biosens. Bioelectron.* **2013**, *48*, 188–196.
26. Pennell, T.; Suchyna, T.; Wang, J.; et al. Microfluidic Chip to Produce Temperature Jumps for Electrophysiology. *Anal. Chem.* **2008**, *80*, 2447–2451.
27. Vukasinovic, J.; Cullen, D. K.; LaPlaca, M. C.; et al. A Microperfused Incubator for Tissue Mimetic 3D Cultures. *Biomed. Microdevices* **2009**, *11*, 1155–1165.
28. Abeille, F.; Mittler, F.; Obeid, P.; et al. Continuous Microcarrier-Based Cell Culture in a Benchtop Microfluidic Bioreactor. *Lab Chip* **2014**, *14*, 3510–3518.
29. Riley, M. Instrumentation and Process Control. In *Cell Culture Technology for Pharmaceutical and Cell-Based Therapies*; Ozturk, S., Hu, W., Eds.; CRC Press: Boca Raton, FL, 2005; pp 249–297.
30. Biffi, E.; Regalia, G.; Ghezzi, D.; et al. A Novel Environmental Chamber for Neuronal Network Multisite Recordings. *Biotechnol. Bioeng.* **2012**, *109*, 2553–2566.
31. Lin, J.-L.; Wu, M.-H.; Kuo, C.-Y.; et al. Application of Indium Tin Oxide (ITO)-Based Microheater Chip with Uniform Thermal Distribution for Perfusion Cell Culture Outside a Cell Incubator. *Biomed. Microdevices* **2010**, *12*, 389–398.
32. Regalia, G.; Biffi, E.; Achilli, S.; et al. Development of a Bench-Top Device for Parallel Climate-Controlled Recordings of Neuronal Cultures Activity with Microelectrode Arrays. *Biotechnol. Bioeng.* **2016**, *113*, 403–413.
33. Buhler, H.; Adamietz, R.; Abeln, T.; et al. Automated Multichamber Time-Lapse Videography for Long-Term in Vivo Observation of Migrating Cells. *In Vivo (Brooklyn)*. **2017**, *31*, 329–334.
34. Liu, L.; Peng, S.; Wen, W.; et al. Micro Thermoindicators and Optical-Electronic Temperature Control for Microfluidic Applications. *Appl. Phys. Lett.* **2007**, *91*, 93513.
35. Glawdel, T.; Almutairi, Z.; Wang, S.; et al. Photobleaching Absorbed Rhodamine B to Improve Temperature Measurements in PDMS Microchannels. *Lab Chip* **2009**, *9*, 171–174.
36. Ross, D.; Gaitan, M.; Locascio, L. E. Temperature Measurement in Microfluidic Systems Using a Temperature-Dependent Fluorescent Dye. *Anal. Chem.* **2001**, *73*, 4117–4123.
37. Samy, R.; Glawdel, T.; Ren, C. L. Method for Microfluidic Whole-Chip Temperature Measurement Using Thin-Film Poly (Dimethylsiloxane)/ Rhodamine B. *Measurement* **2008**, *80*, 4117–4123.
38. Mäki, A.-J.; Rynänen, T.; Verho, J.; et al. Indirect Temperature Measurement and Control Method for Cell Culture Devices. *IEEE Trans. Autom. Sci. Eng.* **2016**, No. 99, 1–10.
39. Rajan, D. K.; Kreutzer, J.; Välimäki, H.; et al. A portable live-cell imaging system with an invert-upright-convertible architecture and a mini-bioreactor for long-term simultaneous cell imaging, chemical sensing and electrophysiological recording. *IEEE Access*, in press.

40. Kreutzer, J.; Ylä-Outinen, L.; Kärnä, P.; et al. Structured PDMS Chambers for Enhanced Human Neuronal Cell Activity on MEA Platforms. *J. Bionic Eng.* **2012**, *9*, 1–10
41. Kreutzer, J.; Ylä-Outinen, L.; Mäki, A.-J.; et al. Cell Culture Chamber with Gas Supply for Prolonged Recording of Human Neuronal Cells on Microelectrode Array. *J. Neurosci. Methods* **2017**, *280*, 27–35.
42. Lahti, A. L.; Kujala, V. J.; Chapman, H.; et al. Model for Long QT Syndrome Type 2 Using Human iPS Cells Demonstrates Arrhythmogenic Characteristics in Cell Culture. *Dis. Model. Mech.* **2012**, *5*, 220–230.
43. Kiviahio, A. L.; Ahola, A.; Larsson, K.; et al. Distinct Electrophysiological and Mechanical Beating Phenotypes of Long QT Syndrome Type 1-Specific Cardiomyocytes Carrying Different Mutations. *IJC Hear. Vasc.* **2015**, *8*, 19–31.
44. Ahola, A.; Kiviahio, A. L.; Larsson, K.; et al. Video Image-Based Analysis of Single Human Induced Pluripotent Stem Cell Derived Cardiomyocyte Beating Dynamics Using Digital Image Correlation. *Biomed. Eng. Online* **2014**, *13*, 39.
45. Penttinen, K.; Swan, H.; Vanninen, S.; et al. Antiarrhythmic Effects of Dantrolene in Patients with Catecholaminergic Polymorphic Ventricular Tachycardia and Replication of the Responses Using iPSC Models. *PLoS One* **2015**, *10*, 1–17.
46. van Schijndel, A. Integrated Heat Air and Moisture Modeling and Simulation. Ph.D. Thesis. Technische Universiteit Eindhoven, Eindhoven, May 2007.
47. Ljung, L. Convergence Analysis of Parametric Identification Methods. *IEEE Trans. Automat. Contr.* **1978**, *23*, 770–783.
48. Ljung, L. *System Identification Toolbox User's Guide*, 9.4th edition. The MathWorks, Inc.: Natick, MA, 2016.
49. Bridle, H.; Millingen, M.; Jesorka, A. On-Chip Fabrication to Add Temperature Control to a Microfluidic Solution Exchange System. *Lab Chip* **2008**, *8*, 480.
50. Björk, S.; Ojala, E. A.; Nordström, T.; et al. Evaluation of Optogenetic Electrophysiology Tools in Human Stem Cell-Derived Cardiomyocytes. *Front. Physiol.* **2017**, *8*, 884.
51. Ahola, A.; Pölönen, R.-P.; Aalto-Setälä, K.; et al. Simultaneous Measurement of Contraction and Calcium Transients in Stem Cell Derived Cardiomyocytes. *Ann. Biomed. Eng.* **2018**, *46*, 148–158.
52. Hsieh, C.-C.; Huang, S.-B.; Wu, P.-C.; et al. A Microfluidic Cell Culture Platform for Real-Time Cellular Imaging. *Biomed. Microdevices* **2009**, *11*, 903–913.
53. Huang, S.-B.; Wang, S.-S.; Hsieh, C.-H.; et al. An Integrated Microfluidic Cell Culture System for High-Throughput Perfusion Three-Dimensional Cell Culture-Based Assays: Effect of Cell Culture Model on the Results of Chemosensitivity Assays. *Lab Chip* **2013**, *13*, 1133.
54. Lin, L.; Wang, S.-S.; Wu, M.-H.; et al. Development of an Integrated Microfluidic Perfusion Cell Culture System for Real-Time Microscopic Observation of Biological Cells. *Sensors* **2011**, *11*, 8395–8411.
55. Yamamoto, T.; Fujii, T.; Nojima, T. PDMS–glass Hybrid Microreactor Array with Embedded Temperature Control Device. Application to Cell-Free Protein Synthesis. *Lab Chip* **2002**, *2*, 197–202.
56. Witte, H.; Stubenrauch, M.; Fröber, U.; et al. Integration of 3-D Cell Cultures in Fluidic Microsystems for Biological Screenings. *Eng. Life Sci.* **2011**, *11*, 140–147
57. Nieto, D.; McGlynn, P.; de la Fuente, M.; et al. Laser Microfabrication of a Microheater Chip for Cell Culture Outside a Cell Incubator. *Colloids Surfaces B Biointerfaces* **2017**, *154*, 263–269.

58. Cheng, J. Y.; Yen, M. H.; Kuo, C. Te; et al. A Transparent Cell-Culture Microchamber with a Variably Controlled Concentration Gradient Generator and Flow Field Rectifier. *Biomicrofluidics* **2008**, 2, 024105.
59. Kienast, R.; Stöger, M.; Handler, M.; et al. Alterations of Field Potentials in Isotropic Cardiomyocyte Cell Layers Induced by Multiple Endogenous Pacemakers under Normal and Hypothermal Conditions. *Am. J. Physiol. - Hear. Circ. Physiol.* **2014**, 307, H1013-23.
60. Weisser, J.; Martin, J.; Bisping, E.; et al. Influence of Mild Hypothermia on Myocardial Contractility and Circulatory Function. *Basic Res. Cardiol.* **2001**, 96, 198–205.
61. Välimäki, H.; Verho, J.; Kreutzer, J.; et al. Fluorimetric Oxygen Sensor with an Efficient Optical Read-out for in Vitro Cell Models. *Sensors Actuators B Chem.* **2017**, 249, 738–746.
62. Demming, S.; Peterat, G.; Llobera, A.; et al. Vertical Microbubble Column-A Photonic Lab-on-Chip for Cultivation and Online Analysis of Yeast Cell Cultures. *Biomicrofluidics* **2012**, 6, 034106.
63. Schindler, M.; Nur-E-Kamal, A.; Ahmed, I.; et al. Living in Three Dimensions. *Cell Biochem. Biophys.* **2006**, 45, 215–227.

FIGURES

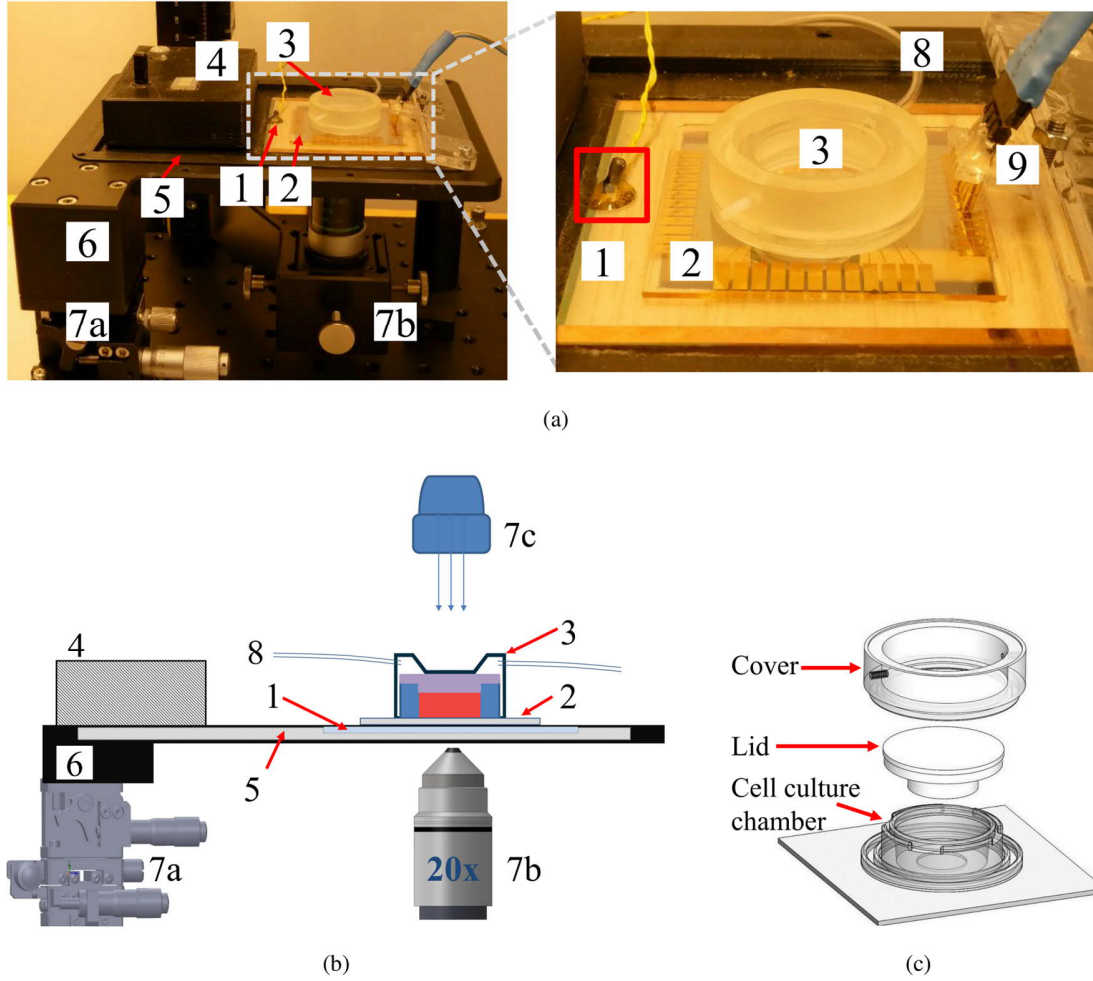


Figure 1. A Portable Microscale Cell Culture System. Numbers show the 1) ITO heater, 2) temperature sensor plate (TSP), 3) cell culture device, 4) electronics, 5) ITO frame, 6) aluminum frame, 7a) xyz-stage, 7b) motorized inverted microscopy with 20x objective, 7c) illumination unit using white LED, 8) gas supply, and 9) connection pins to read resistances of TSP sensors. (a) Experimental setup. The Pt100 sensor measuring temperature of the ITO heater (T_{ITO}) is marked with a red rectangle. (b) The schematic of the optical system tailored for cell culturing. Parts 7a-c are part of the invert-upright convertible 20X microscopy system that has been previously presented.³⁹ (c) Expanded view of the cell culture device presenting the cell culture chamber, the lid, and the cover. The assembled device on the TSP is shown in Fig. 1(a).

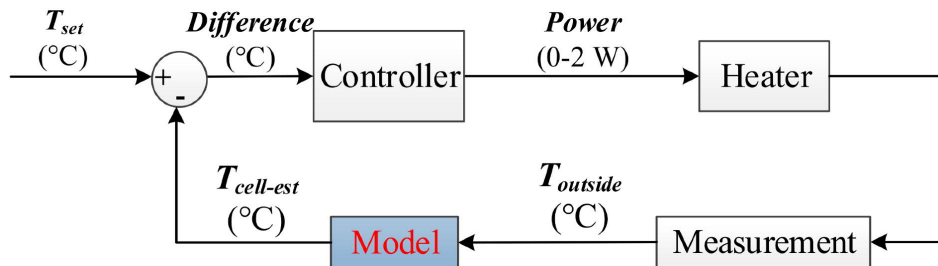


Figure 2. Working principle of indirect cell culture temperature measurement and control.

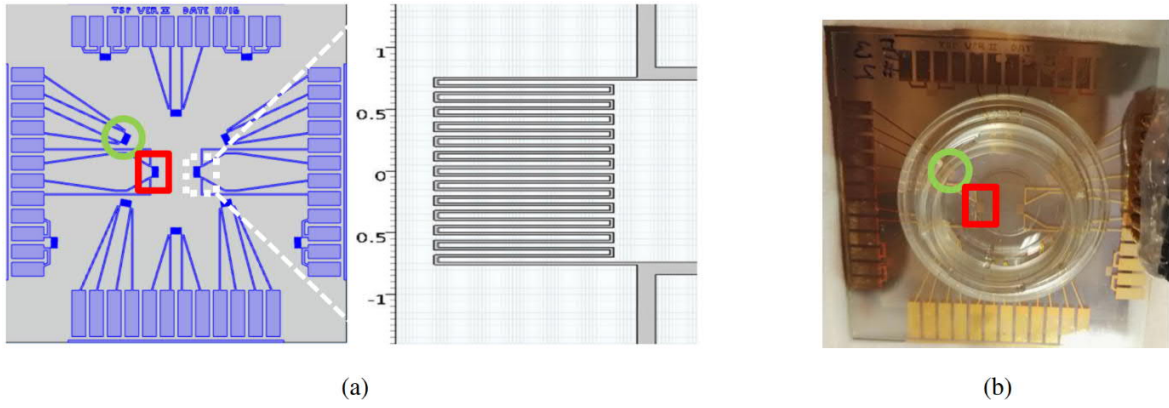


Figure 3. Temperature logging: (a) designed sensor layout and (b) temperature sensor plate together with cell culture chamber. The resistors marked with a red square and a green circle are used to measure T_{cell} and T_{TSP} , respectively.

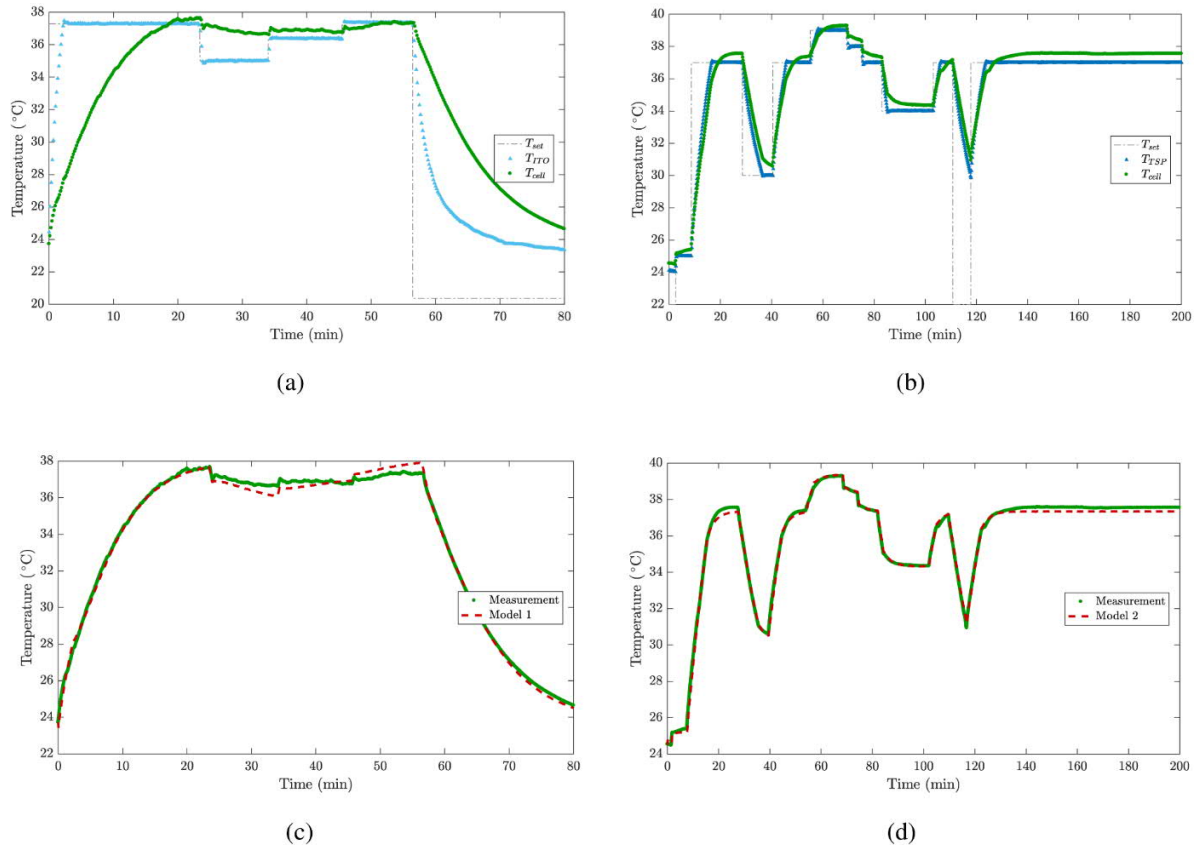


Figure 4. Model development: model estimation experiments for (a) Model 1 and (b) Model 2, and comparison of measured cell culture temperature and model estimate using (c) Model 1 and (d) Model 2.

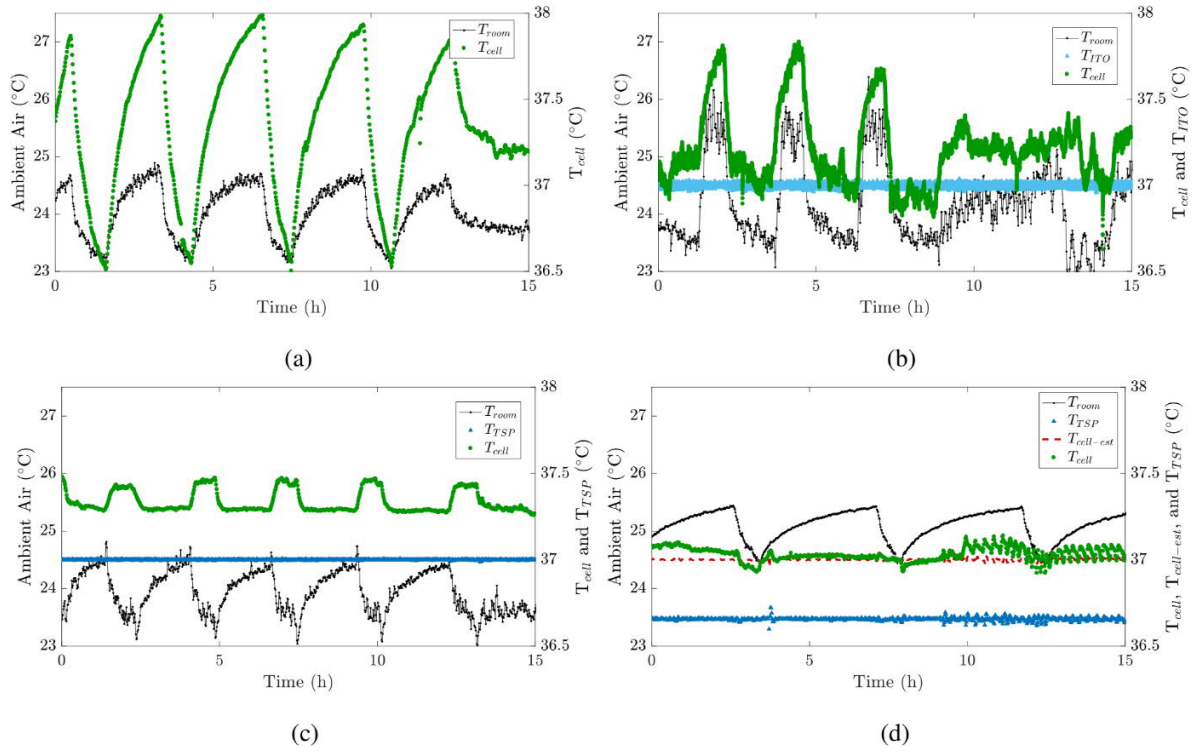


Figure 5. Comparison of the different temperature controller strategies: (a) open-loop system with a constant power, closed-loop systems where temperature is controlled by (b) T_{ITO} , (c) T_{TSP} , and (d) $T_{cell-est}$ calculated by T_{TSP} and Model 2.

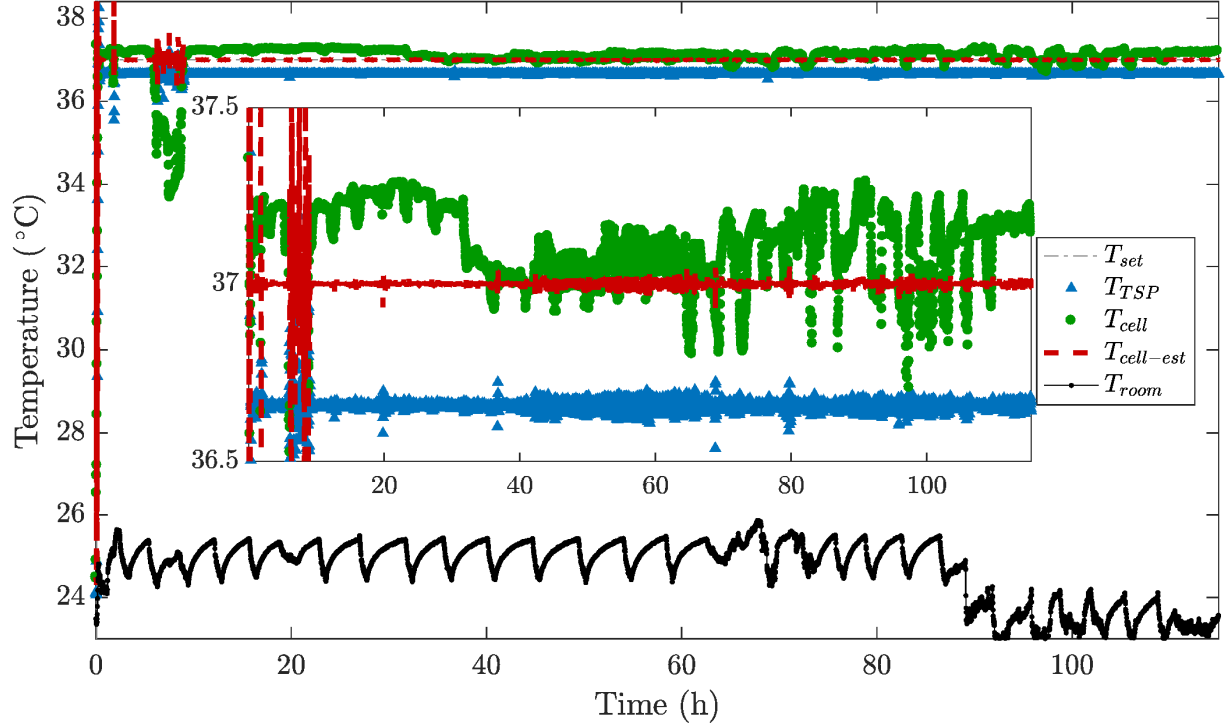


Figure 6. Long-term temperature control using Model 2.

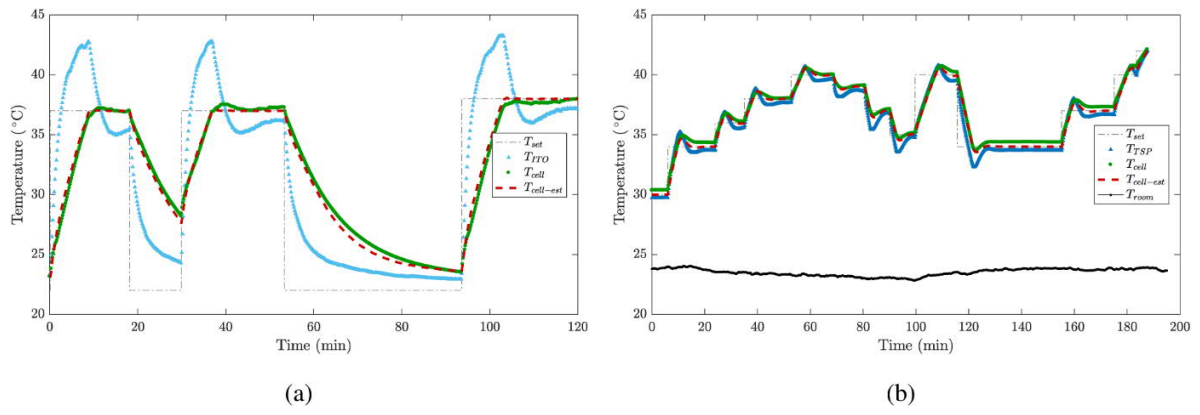


Figure 7. Transient temperature control using (a) Model 1 and (b) Model 2.

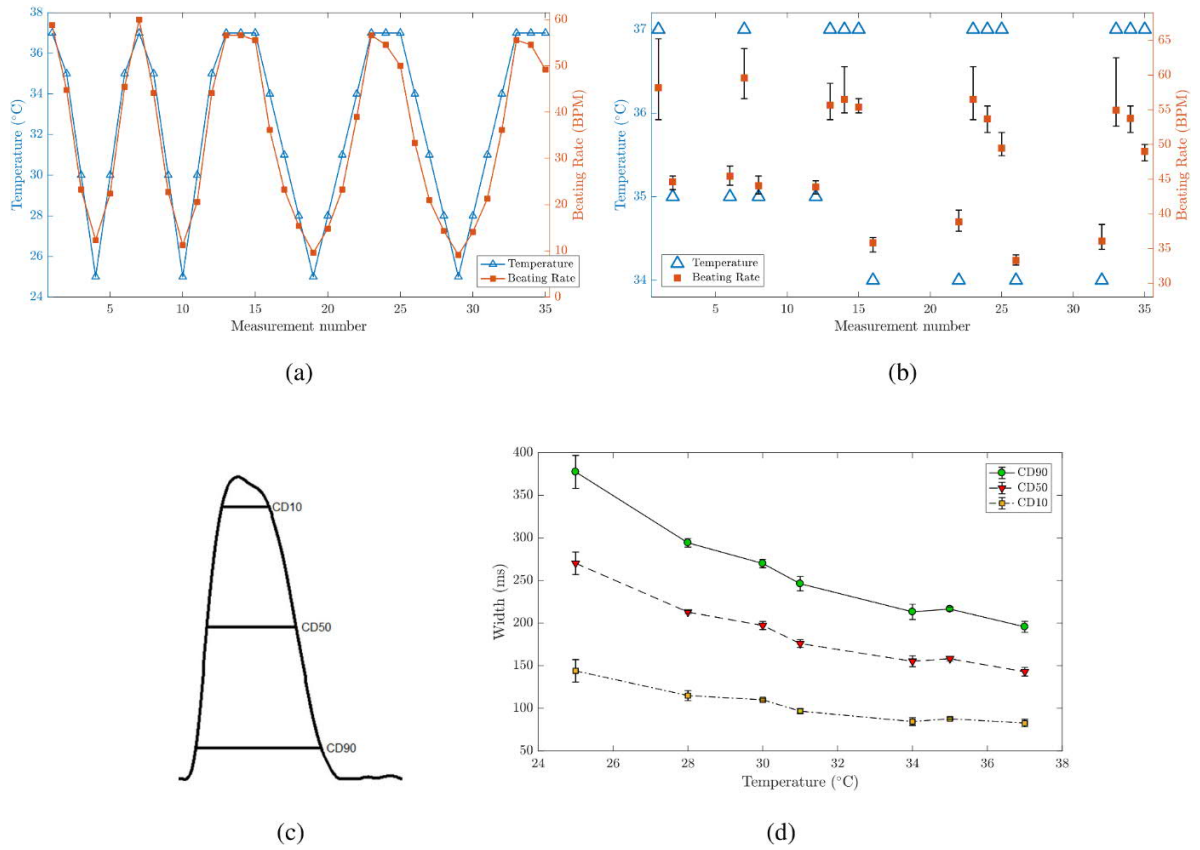


Figure 8. Study of beating cardiomyocytes in different temperatures. (a) Beating rate of the cardiomyocytes in different temperatures and (b) a zoomed in image showing the average beating rates at temperatures between 34 °C and 37 °C. Error bars represent the minimum and maximum values calculated from each 60 s video. (c) Definition of contraction duration widths at three height levels from the peak maximum and (d) averages and standard deviations of the contraction durations in different temperatures.